Corrosion of an Active Antibacterial Nanostructured Coating on Titanium

DANIELA IONITA, LUIZA NECULA, MARIANA PRODANA*, GEORGETA TOTEA, IOANA DEMETRESCU
University Politehnica of Bucharest, Faculty of Applied Chemistry and Materials Science, 1-7 Polizu Str., 011061, Bucharest, Romania

This study aims on antibacterial and corrosion characterization of a complex ceramic coating based on titania (TiO_2) nanotubes, hydroxyapatite (HA) and single walled carbon nanotubes (SWCNTs), in physiological environment. Hybrid materials structure was identified by Fourier transformed infrared spectroscopy (FTIR) and their surface analysed by scanning electron microscopy (SEM) and contact angle analysis. The most hydrophilic sample was the one with TiO_2-HA coating. The electrochemical behavior of materials has been investigated in Ringer solution performing potentiodiynamic polarization and electrochemical impedance spectroscopy. Antibacterial properties of coatings were determined by contact method using two types of strains, one of them Staphylococus aureus (S. aureus) is a positive gram bacteria and another one Pseudomonas aureoginosa (P. aureoginosa) a negative gram bacteria. The corrosion rates are in the perfect stable domain of corrosion resistance and no breakdown phenomena were observed. A range of stability in tested bioliquid has been established from electrochemical and ICP-MS measurements. TiO_2-HA-SWCNTs coating has the best corrosion resistance and the best barrier properties for ions release. Antibacterial effect of TiO_2-HA-SWCNTs coating seems to be synergistic being higher compared to TiO_2 nanotubes and TiO_2-HA coating.

Keywords: antibacterial effect, titania nanotubes, hydroxyapatite, SWCNTs, corrosion

The corrosion of coated and uncoated titanium and its alloys in bioliquids was subject of a large number of papers [1-3]. One of the most studied ceramic coatings with diversified biomedical applications is hydroxyapatite (HA, $Ca_{10}(PO_4)_6(OH)_2$) with the ratio of Ca/P of 1.67, the major mineral component of the bone, being also the cheapest solution for bone grafts, maxillofacial surgeries, dentistry bone defects repair in orthopaedic interventions [4]. Bone consists of an organic phase - collagen up to 30 wt%, an inorganic phase almost 70 wt% and around 10 wt% of water [5]. The bare hydroxyapatite has own important properties, such as: low weight, tensile and fatigue strength [6], no side effects on human organism [7] and bioactive properties. It has the capability to form strong chemical bonds with surrounding bone living tissues [8], has osteogenic potential to promote bone growth and to promote metallic implant integration with host bone. The hydroxyapatite can be obtained by different methods: from natural sources or *via* chemical synthesis [9].

However, despite all the merits of hydroxyapatite regarding chemical and phase composition which is a strong recommendation as a biocompatible ceramic material, its mechanical low strength is a major disadvantage. The intrinsec brittleness and low wear resistance of hydroxyapatite do not allow the use of it in long term implant applications. A solution to this problem is a second phase material reinforcement. A possibility mentioned in the literature should be the biodegradable polymers [10] and other possibilities are the reinforcement with zirconia [11], glass [12] or carbon structures [13]. The carbon structures as nanotubes present significant antibacterial effect [14] and are very promissing in various hybrid combination.

The carbon nanotubes (CNTs) are the most organised known structure of carbon fiber [15]. There exists three common types of carbon nanotubes: single walled nanotubes (SWCNTs), multiwalled nanotubes (MWCNTs) and carbon nanofibres [16]. Carbon nanotubes materials are used in electronics to enhance fibber composites and in medicine applications for drug delivery systems, due to their remarkable properties: mechanical strength, flexibility, high aspect ratio [17], thermal conductivities [18] and low density. The combination of all these unique properties in one material has increased the interest in deploying CNT in a novel ceramic composite system [17].

CNTs have poor dissolution properties that restricts their applications [19]. The nanotubes are held together in bundles by van der Waals forces, but the improved properties of carbon nanotubes could be achieved when CNTs are dispersed in liquid media. CNT dispersion could be a covalent or a noncovalent functionalization. The noncovalent preserves the sp^2 carbon network structure permiting the adsorption of different biomolecules or metallic nanoparticles onto their surface [20].

Having very good mechanical properties as well as corrosion and biological improved properties, the aligned carbon nanotubes containing scaffolds for neural tissue regeneration have been proposed recently for new biomedical applications [21].

Nowadays, we have two principally types of orthopedic biomaterials: implants and scaffolds for tissue regeneration [22]. Titanium and its alloys are the most common used as metal substrate for HA coating, because they have similar mechanichal properties to bones and excellent corrosion resistance [23]. In order to help achieving the necessary qualities in bone implant bonding and implantation longevity for a new bioactive implant with better and safer exploitation the carbon nanotubes were used to improve their bond with the substrate [24]. The results obtained with MWCNTs [25] present clearly the enhancement of properties, but the investigations on

*email: prodana_mariana@yahoo.com; Phone: 0214023930

SWCNTs need more experiments. Up to date, most of the earlier works have utilized the incorporation of one or two components altering the surface of Ti by changing the film native TiO_2 and successfully electrodeposited HA and SWCNTs-HA on the material having TiO_2 nanotubes on the surface [26].

The present work aims and its novelty as well is to investigate the preparation, antibacterial effect and corrosion resistance of a new complex hybrid material based on three components, as TiO_2 nanotubes, hydroxyapatite, and functionalized carbon nanotubes with carboxyl groups (SWCNTs-COOH). The use of functionalised carbon nanotubes reveals the enhancement of their properties [27], especially the antibacterial effect which is a need in our days when bacteria are stronger and stronger and their inactivation on various surfaces is important for biosafety and public health. Electrochemical stability of the new coating was tested in Ringer solution and established by open-circuit potential (OCP), potentiodynamic polarization tests Tafel plots and electrochemical impedance spectroscopy (EIS). Surface energy and ion release determinations in conection with antibacterial activity and hemocompatibility tests have permitted a discussion about bioperformance of the proposed new coating.

Experimental part

We used the folowing materials: SWCNTs, with diameter about 20-40 nm and length of 0.1-10μm (from Sigma Aldrich, 90% purity) titanium plates 99,7% purity (2mm tickness), H_2SO_4, HNO_3, $NH_4H_2PO_4$ and $Ca(NO_3)_2 \cdot 4H_2O$ reagents (from Sigma Aldrich).

The nanotubes functionalization was performed in an aqueous mixture of H_2SO_4:HNO_3 of 2:3 (V:V), for 8 h at 50°C under ultrasonication. The samples were afterwards washed with distilled water and dried at 50°C for 12 h.

The titanium samples were anodised to obtain TiO_2 nanotube for 2 h, at 20V, in an aqueous electrolyte containing NH_4F and ethylene glycol [28]. The electrochemical setup was a two-electrode system with Ti as working electrode and Pt as counter electrode.

For the electrochemical deposition of SWCNTs-HA on TiO_2 nanotubes we used the polarization method for 120 min at -1.4 V vs Ag/AgCl as a reference electrode; the aqueous suspensions contained 1 g/L SWCNT-COOH, 9.91 g/L $Ca(NO_3)_2 \cdot 4H_2O$ and 2.875 g/L $NH_4H_2PO_4$. The cell was placed on a heating and stirring electric stove, at 80°C. The obtained samples were washed after electrodeposition process with distilled water.

TiO_2-HA coatings were obtained using the procedure described above the only difference was that the electrolyte with calcium nitrate and ammonium hypophosphate did not contain carbon nanotubes.

FT-IR spectra were recorded by using a Spectrum 100 Series FT-IR spectrometer from Perkin Elmer in the range 4000-400 cm^{-1}. The hydrophilic/hydrophobic behaviour of TiO_2, TiO_2-HA and TiO_2-HA-SWCNTs materials was investigated using static contact angle measurements, which were performed using 100 Optical Contact Angle Meter - CAM 100, at room temperature. In order to perform this analysis we used distilled water. The nanotubes surface synthesized via anodic oxidation was studied using a scanning electron microscope (SEM), Hitachi SU 8230, equipped with an EDS Oxford detector analyzer. The investigation consisted in conducting secondary electron image in order to observe the morphology of deposits and also EDS analysis to determine the chemical composition of the obtained layers.

A three-electrode cell configuration consisting of our obtained composite as working electrode, a Pt wire as counter electrode and Ag/AgCl as reference electrode was used for electrochemical experiments in Ringer solution (8.6 g/L NaCl, 0.3 g/L KCl, and 0.48 g/L $CaCl_2$). The equipment utilized was Autolab PGSTAT 302N potentiostat/galvanostat with NOVA 10 software. Open circuit potential (OCP) measurements were carried out for short time in order to monitor the potential-time behavior of the electrodes. Potentiodynamic polarizations were conducted in a potential range from -0.25 V to 1 V vs. OCP with a scan rate of 2 mV s^{-1} after immersing the samples in solutions for 30 min. Electrochemical Impedance Spectroscopy (EIS) measurements were carried out at OCP. Impedance measurements were performed from 10^{-2} to 10^5 Hz with an *ac* amplitude of ± 10 mV. The impedance data were analysed with the Zview 2.70 software package and fitted to the corresponding equivalent electrical circuit. Tafel plots were registered between ±300 mV vs free potential at a scan rate of 2 mV s^{-1} and corrosion parameters such as j_{corr} - current density, E_{corr} -corrosion potential, R_p - polarization resistance and v_{corr} - corrosion rate, were evaluated.

The evolution of titanium ions release in time was measured with an inductively plasma mass spectrometer (ICP-MS) equipment Perkin Elmer ELAN DRC-e in the working conditions presented in another work [29]. The antibacterial effect was determined using an UV–Vis Jenway Spectrophotometer, for determination optical density at 600 nm corresponding to the blank, the sample in infected media (T_0 and T_1 at initial time and 24 h) and positive control (C_0 and C_1 at initial time and 24 h). The following equation (1) [30] was applied:

$$I\% = \frac{(C_1 - C_0) - (T_1 - T_0)}{(C_1 - C_0)} \times 100 \quad (1)$$

This equation permits the determination of the growth inhibition index $I_{\%}$ of a negative gram bacteria as P. aeruginosa (ATCC 27853) and a positive gram bacteria as S. aureus (ATCC 25923) respectively.

P. aeruginosa is a well known motile bacteria used as a model microorganism for investigation of chemotactic behaviors in ecosystem and it is responsable for necrosys and osteomelitys [31]. S. Aureus, which is responsible for osteomelitys, was regarded long time as a non-motile organism, but recently [32] it has been shown that it can move across agar surfaces.

According to the procedure described in literature [33] the coating samples were rinsed with distilled water and sterilized at 180°C for 2h, before the antibacterial assay. The concentration was fixed at 0.5 McFarland units measured with a McFarland densitometer. The amount of infected medium added in each sample was 10 mL and took place before incubation at 37°C, for 24h. The blank was represented by saline solution and the positive control was represented by the infected medium without samples, and both of them were kept in the same conditions.

The red cells (RBCs called erytrocytes) have extremely fragile membrane and their destruction followed by cell lysis or aggregation of platelets, have to be investigated in order to see if a material is hemocompatible. We used smear observation to assess the damage caused to the RBC membranes and platelets after exposure of blood to these biomaterials. The blood was collected in sterile condition by veinipunture on EDTA vacuum tubes from a healthy donor, that signed an informed consent regarding the confidentiality data and the use of remainig biological fluid in scientific purpose. Four smears were prepared, one before blood–material interaction and the other three after

30 minutes contact with the samples at 37°C. As staining method for the smears we used the panoptic method [34] of Pappenheim using May-Grunwald-Giemsa stain. A microscope Olympus was used for smear observation. We placed 200 µL of anticoagulated blood on the samples in a Petri dish surrounded with wet cotton pieces, in order to avoid the cells degradation due to dehydration.

Results and discussions

Electrodeposition of coatings

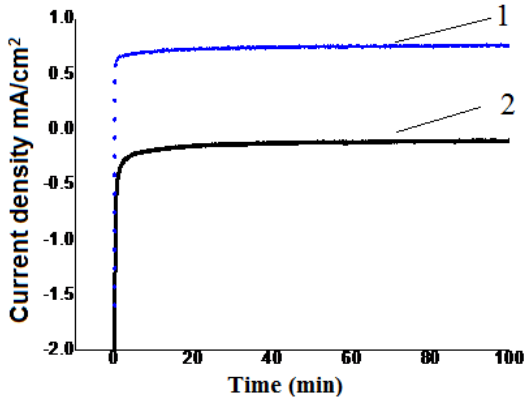

Fig. 1. A comparison of electrolysis current density for potentiostatic deposition of HA (1) and SWCNTs (2) onto TiO_2 coating on titanium substrate

In figure 1 it can be observed an approximate 1 mA/cm^2 difference in the transitory current density of HA and SWCNTs-HA onto TiO_2 on titanium plates which is possibly due to the insulator character of HA vs. the conductive character of SWCNTs composite. During the electro-deposition of hybrid coating we could notice the signal division in two parts: a rapid current increase due to the new active sites deposition, and finally a constant current behaviour due to the growing processes on titanium surface.

Surface characterisation

The structure surfaces of samples were identified by using FT-IR spectroscopy. Figure 2 represents the spectra for both TiO_2-HA and TiO_2-HA-SWCNT$_S$ samples. These spectra confirmed the formation of apatite phase in all coatings. The bands at around 986 cm^{-1} and 1056 cm^{-1} correspond to the stretching and wagging vibrations of the PO_4^{3-} group, and the bands at around 3474 cm^{-1} correspond to the OH^- bands. The stretching vibration of carbonate band was observed at 1646 cm^{-1}. In the region of 2395 cm^{-1} the stretching vibration of the adsorbed carbon dioxide is present [25]. The functionalization of SWCNT$_S$ forming the -COOH groups on their surface deternines the development a specific peaks. The band around 1641 cm^{-1} can be attributed to carbonyl C=O groups, while the band around 1117 cm^{-1} can be assigned to C-O groups [35].

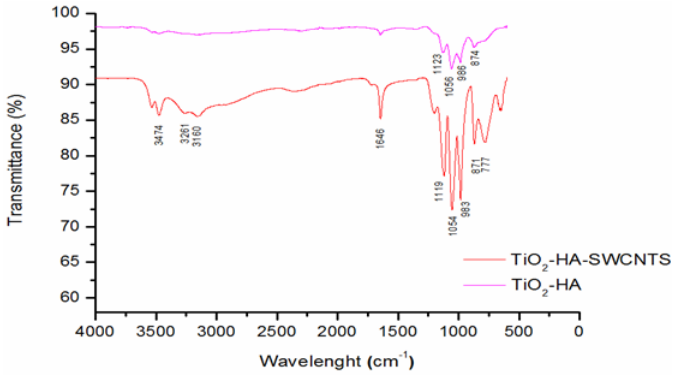

Fig. 2. FTIR spectra of both TiO_2-HA and TiO_2-HA-SWCNTs materials

SEM analysis

In figure 3 are presented SEM micrographs and EDS spectra for all deposits; for TiO_2 sample we can observe the morphology of TiO_2 nanotubes. For this coating sample the TiO_2 nanotubes are arranged on strings, with nanotubes diameter between 10-30 nm. EDS spectra were used to show the obtained titanium and oxygen peaks. For TiO_2-HA-SWCNTs sample, the Ca/P deposition ratio is 1.27. The EDS spectra proved the presence of Ti, Ca, P and C peaks. The calcium phosphates groups have platelet and needle-like forms. The diameters of needles are between 50-100 nm and platelet shape width is almost 300 nm. The length both formations length is between 0.2 and 5 µm. Regarding TiO_2-HA sample, the EDS spectra showed Ti, Ca and P peaks. The Ca/P deposition ratio is 1.30, a little higher that for the second sample. We can notice needle shapes with the thickness between 0.1-0.2 µm and platelet shape with the width between 0.3 -0.8 µm. For both shapes the length is less than 5 µm. Table 1 summarizes the appearance of C element in TiO_2-HA-SWCNTs sample, which is due the SWCNTs-COOH incorporated into HA matrix.

Contact angle determinations

The contact angle values are represented in table 2 together with the surface energy values evaluated from the surface energy ξ which was computed using equation (2).

$$\xi = \gamma \cos\theta, \qquad (2)$$

where θ is the contact angle and γ = 72.8 mN·m^{-1} experimentally determined surface energy for water. All the surfaces of the samples have surface energy values between 43.56 and 71.68 mN·m^{-1}. Because the values are higher than 30 mN·m^{-1}, such values indicate bioadhesion [36, 37] and a positive cell response [38].

a		b		c	
Elements	Atomic %	Elements	Atomic %	Elements	Atomic %
O	60.15	O	72.00	C	3.80
F	7.19	P	12.24	O	66.40
Ti	30.01	Ca	15.75	P	12.96
C	2.65	Ti	0.01	Ca	16.49
				Ti	0.35
Total	100		100		100

Table 1
QUANTITATIVE ANALYSIS FOR (a) TiO_2, (b) TiO_2-HA, (c) TiO_2-HA-SWCNTs SAMPLES

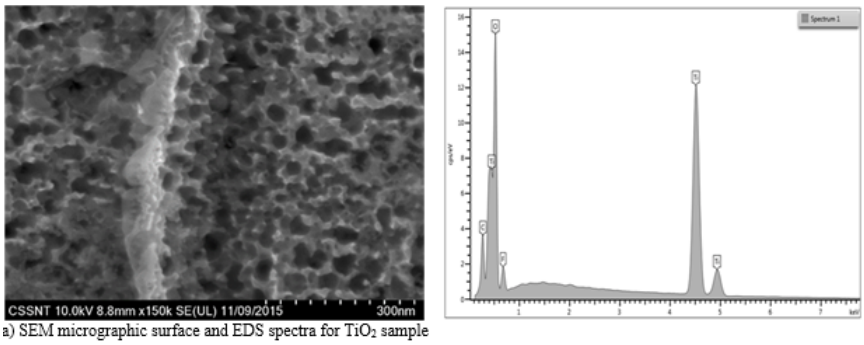

a) SEM micrographic surface and EDS spectra for TiO_2 sample

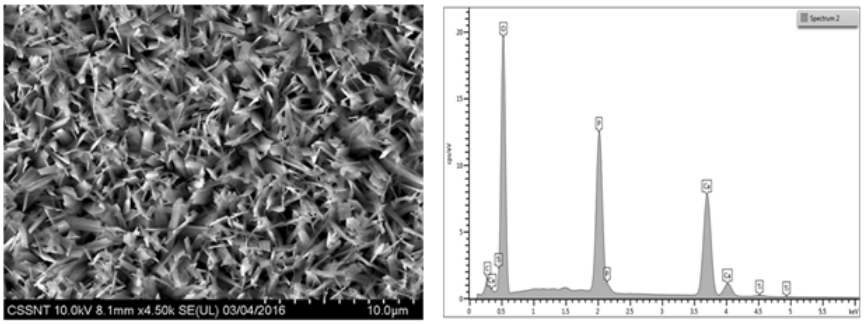

b) SEM micrographic surface and EDS spectra for TiO_2 -HA-SWCNTs sample

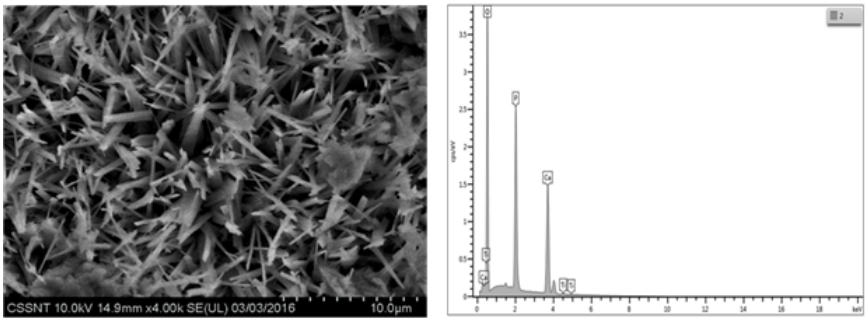

c) SEM micrographic surface and EDS spectra for sample TiO_2-HA sample

Fig. 3. Morphologies of samples and the EDS spectra

Sample	Contact angle values	Surface energy ($mN \cdot m^{-1}$)
TiO_2	53.25	43.56
TiO_2-HA	10.05	71.68
TiO_2-HA -SWCNTs	13.37	70.83

Table 2
CONTACT ANGLE VALUES AND SURFACE ENERGY FOR TiO_2, TiO_2-HA AND TiO_2-HA-SWCNT$_S$ SAMPLES

The less hydrophilic sample was TiO_2 sample, while the others two samples showed a hydrophilic behaviour. The most hydrophilic sample is TiO_2-HA as a consequence of HA presence. The hydrophilic behaviour can be observed for all our samples due to the values of contact angles which are smaller than 90°. Comparing with the results obtained previously with the coating TiO_2-HA-MWCNTs [25] it is worth to mention that in the present case the hydrophilic character of TiO_2-HA-SWCNT$_S$ is much stronger, the contact angle being pretty close to the value for TiO_2-HA. The surface energy of TiO_2-HA-SWCNTs has a close value as for TiO_2-HA, as well.

Electrochemical behaviour of samples in Ringer solution

In all cases, the initial OCP value shifts continuously towards the positive direction of potential, first with a faster rate and then slowly until it reaches an almost quasi-stationary state. For reaching the steady state for the titanium coated with TiO_2 180 min time is requiered whereas, for titanium coated with TiO_2- HA this time is 105 min, and for Ti coated with TiO_2-HA-SWCNT$_S$ only 30 min was necessary. The values of potential for the samples at steady state were: -0.25, -0.05 and +0.095 V/AgCl respectively. Nevertheless, all these potentials are found in the stability region of TiO_2 oxide in the Ti-H_2O Pourbaix diagram for aqueous solutions of *p*H 5.5 [39].

Figure 4 presents the potentiodynamic polarization curves in a narrow range of potentials from all samples in

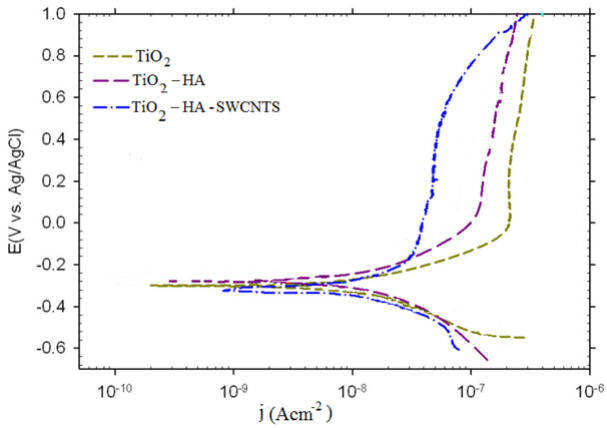

Fig. 4. Potentiodynamic polarization curves for TiO_2, TiO_2 –HA, TiO_2-HA-SWCNT$_S$ materials in Ringer solution at 37°C

Table 3
THE ELECTROCHEMICAL PARAMETERS OBTAINED BY EXTRAPOLATION OF TAFEL CURVES FOR ALL THREE COATED MATERIALS IN RINGER SOLUTION

Sample	E_{cor} [V]	j_{corr} [A·cm^{-2}]	Corrosion rate [mm/year]	Polarization resistance [Ω]
TiO_2	-0.495	$7.98 \cdot 10^{-8}$	$2.77 \cdot 10^{-3}$	$1.129 \cdot 10^{5}$
TiO_2-HA	-0.343	$8.01 \cdot 10^{-8}$	$2.78 \cdot 10^{-3}$	$0.865 \cdot 10^{5}$
TiO_2-HA-SWCNTS	-0.325	$2.90 \cdot 10^{-8}$	$1.01 \cdot 10^{-3}$	$1.573 \cdot 10^{5}$

Ringer solution at 37°C. From the diagram it can be noticed that the TiO_2-HA-$SWCNT_S$ material has the best corrosion resistance in this case, due to the smallest values of the current density (j_{corr}). Table 3 shows the determined values of corrosion potential (E_{corr}), corrosion current (j_{corr}), polarisation resistance and corrosion rate expressed in mm/year.

The cathodic polarization behaviour of samples was similar meaning that the cathodic behaviour is due to reduction of oxygen. A breakdown potential was not detected for any of the samples up to 1 V. It can be noted that the passive current density of samples decreased in the following order: TiO_2 > TiO_2-HA > TiO_2-HA-$SWCNT_S$. This is evidence that the complex coating (TiO_2-HA-$SWCNT_S$) induces an increased stability of the sample. Also, for the samples covered with TiO_2-HA-$SWCNT_S$ the passive domain started at a lower current density (about 10^{-8} A cm^{-2}) compared to samples covered with TiO_2-HA, or TiO_2 (about10^{-7} Acm^{-2} for both)

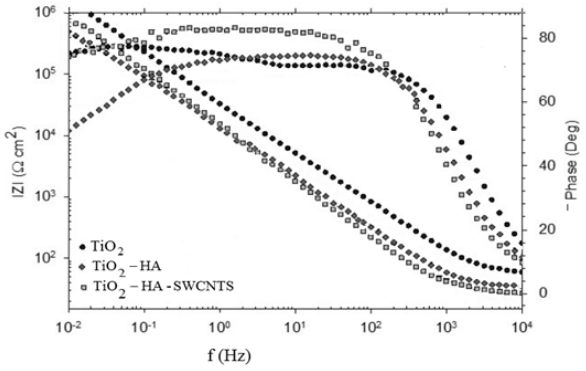

Fig. 5. Bode diagrams for TiO_2, TiO_2-HA, TiO_2-HA-SWCNTs in Ringer solution

The impedance modulus data (fig. 5) for all samples was independent of frequency from 10^4 to 10^3 Hz. In this frequency range the system showed a resistive behaviour corresponding to the solution resistance between the working and reference electrode. The phase angle values reached the maximum value (-80^0) for the samples covered with TiO_2-HA-$SWCNT_S$ at a frequency range from 800 to 0.1 Hz. In this frequency range the sample showed a capacitive behaviour. For the frequency range in which the phase angle values were independent of frequency while the impedance modulus values were increasing, the samples show a passive behavior. When the impedance increased, the phase angle shifted to the lower values by decreasing the frequency from 0.1 to 0.01 Hz.

The impedance can be characterized by a large semicircle capacitive loop and the Nyquist curves showed a one-time constant (fig. 6).

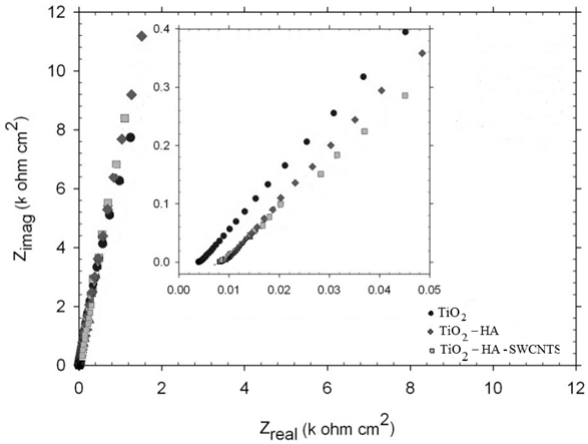

Fig. 6. Nyquist diagrams for TiO_2, TiO_2-HA, TiO_2-HA-$SWCNT_S$ in Ringer solution

The EIS data were fitted by using a simple Randles equivalent circuit (R_S (Rb CPE)) drawn in figure 7. In this circuit, R_S is designated as the Ringer solution resistance between the working and the reference electrode and Rb is the resistance of the barier layer and. A constant phase element (CPE) is used instead of pure capacitor to consider the non-uniform current distribution due to surface roughness and non-homogeneities [38]. The electrochemical characterization of titanium in contact with simulated body fluid under infection conditions was discussed in [39]. The impedance of a constant phase element (Z_{CPE}) is:

$$Z_{CPE} = \frac{1}{(j\omega)^{n_c} Y_0} \quad (3)$$

In equation (3) n_c is an exponent related to deviation between real capacitance and pure capacitance, Y_0 is the general admittance function, and ω represents the angular frequency.

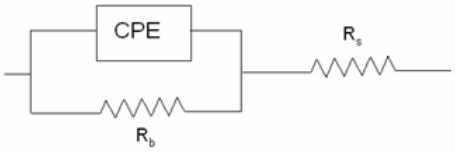

Fig. 7. Equivalent circuit used for fitting the EIS data

The obtained parameters of the electric circuit components along with the chi-square value (c^2) are shown in table 4.

ICP-MS determinations

The evolution of titanium ion release in time from samples immersed in Ringer solution for 3 h is presented in table 5. As can be seen from this table the amount of released Ti is much smaller for the sample with the complex coatings indicating that the coatings act as a barrier inhibiting the ion release.

Antibacterial effect and hemocompatibility test

In table 6 the bacteria growth inhibition rate for the three samples is presented. As can be seen TiO_2 nanotubes, which are known for their effect of increasing biocompatibility, have the smallest action on bacteria inhibition for both tested strains. The inhibition values which are close to each other are a bit higher for S. aureus compared to P. aeroruginosa. For the coatings with TiO_2-HA and TiO_2-HA-SWCNTs the inhibitions are much higher, the most significant being for the sample with SWCNTs well known for their toxicity [35].

Regarding antibacterial mechanism of action it is to mention the general mechanism [36, 37] with two stages as following: an instantaneous and physical reversible

	R_s [$\Omega \cdot cm^2$]	R_b [$k\Omega \cdot cm^2$]	Y_0 [$\mu\Omega^{-1}s^n cm^{-2}$]	n_c	$\chi^2 \cdot 10^4$
TiO_2	8.6	162.4	108.2	096	4.87
TiO_2-HA	9.1	295.6	52.8	0.84	6.75
TiO_2-HA-SWCNTs	9.4	350.8	46.7	0.93	2.68

Table 4
VALUE OF CIRCUIT PARAMETERS OBTAINED FROM EIS FITTING DATA

Table 5
TITANIUM RELEASE FOR THE SAMPLES IMMERSED IN RINGER SOLUTIONS

Coating	Ti concentration (ppb)
TiO_2	12.19
TiO_2/HA	6.98
TiO_2/HA/SWCNTs	5.36

Table 6
ANTIBACTERIAL INHIBITION INDEX

I%	TiO_2	TiO_2-HA	TiO_2-HA-SWCNTs
P.aeruginosa	15.45	42.25	47.55
S. aureus	16.34	50.15	56.53

phase, and a time-dependent irreversible molecular and cellular second phase. At the contact with a support as tissue, a competition between microbial colonization and tissue integration is taking place.

Accordig to literature [37, 38] the materials with surface energies higher that 30 $mN \cdot m^{-1}$ tend to present a greater bioadhesion. Our samples have values higher than 30 $mN \cdot m^{-1}$ presenting significant bioadhesion. As it is well known, the gram-positive bacteria were much more difficult to destroy, due to the more complicated cell wall structure consisting of several layers of peptidoglycan which are thicker as compared to gram-negative bacteria where their cell wall is composed of a single peptidoglycan layer [40-42].

Motility being a key characteristic for bacteria behavior in biofilm formation and host colonization, the difference in motility of S. aureus (which has a more passive motility, but presents spreading and even gliding) compared to P. aeroruginosa could be a reason for the difference in inhibition values. SWCNTs possess important antimicrobial properties [14, 41] even in small amounts, due to the efficient contact with the surface of bacteria cell by hydrophobic interactions, resulting in perturbation of bacterial cell integrity and then cell membrane damage. Cell membrane damage resulting from direct contact with SWCNTs is the likely mechanism, leading to bacterial cell death [43, 44]. The mechanism of antimicrobial activity of SWCNTs is associated also with their dimensions, which influence piercing and wrapping on the lysis of bacterial walls, inducing release of DNA and RNA and leading to destruction of microorganism [45-48].

Regarding hemocompatibility aspect, the blood is the most important body fluid contacting with implantable devices, so its compatibility is of crucial importance in all clinical invasive procedures. As can be seen in figure 8 with blood smears before contact with samples (a, b and c) and after contact figure 8 (d, e and f) the red blood cells membranes remained intact and no signs of hemolysis or dramatic modification of cells shape were seen after incubation. Also for platelets, no signs of aggregations occurred in all three cases. The RBCs on treated samples with TiO_2-HA and TiO_2-HA-$SWCNT_S$ look almost similar to figure 9 a. Such fact is due probably to the values of contact angle close to each other.

Blood compatibility ofbiomaterials is influenced by both surface chemistry and topography. Recently, with the development in nanotechnology, the nanomaterials for bioapplications were developed and the important role of wettability was more investigated. Such approach and results are in accordance with those obtained in the present study.

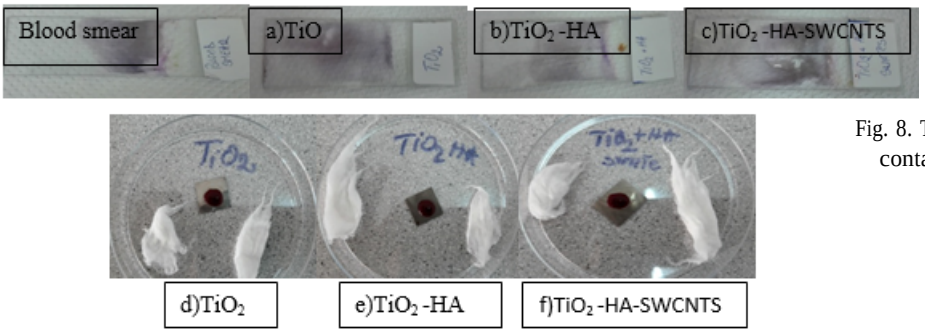

Fig. 8. The first row blood smears before sample contact with blood for: (a) TiO_2; (b) TiO_2-HA; (c) TiO_2-HA-SWCNTs

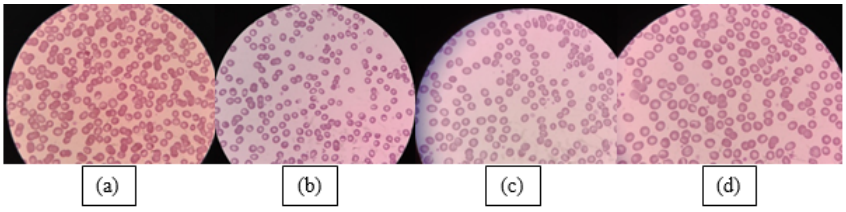

Fig. 9. Images of Petri dishes with RBC after sample contact with blood (a) control (b) TiO_2; (c) TiO_2-HA; (d) TiO_2-HA-SWCNTs

Conclusions

Biofilm embedded bacterial pathogens, such as S. aureus and P. aeruginosa, are major sources of bacterial infections and more and more difficult to be eradicated. Investigation from this paper could be useful for development future coatings able to prevent infections. On this research we studied the antibacterial effect and corrosion of a new composite TiO_2-HA-SWCNTs versus TiO_2-HA obtained by electrodeposition and versus TiO_2. The samples structures were identified using FTIR analysis. From the corrosion tests in Ringer solution and ICP-MS determinations we demonstrated that TiO_2-HA-SWCNTs material has the best corrosion resistance and barrier properties for ions release. This coating has the most significant index of bacteria inhibition for both tested bacteria S. aureus and P. aeruginosa. The best stability in bioliquids and best antibacterial effect recommend such coating for bioapplications in medicine and biotechnology.

Acknowledgements: The work has been funded by the Sectoral Operational Programme Human Resources Development 2007-2013 of the Ministry of European Funds through the Financial Agreement POSDRU/159/1.5/S/134398.

References

1.DILEA, M., MAZARE, A., IONITA, D., DEMETRESCU, I., Mater. Corros., **64**, 2013, p. 493.
2.ICHIM, L., SBARCEA, B.G., PATROI, D., DUMITRIU, C., Rev. Chim.(Bucharest), **67**, no. 11, 2016, p. 2198.
3.IONITA, D., GRECU, M., UNGUREANU, C., DEMETRESCU, I., J. Biosci. Bioeng., **112**, no. 6, 2011 p. 630.
4.DUMITRIU, C., POPESCU, M., VOICU, G., DEMETRESCU, I., Rev. Chim. (Bucharest), **64**, no. 6, 2013, p. 599.
5.DOROZHKIN, S.V., Materials, **2**, no.2, 2009, p. 399.
6.SOBIESZCZYK, S., KLOTZKE, R., Adv. Mater. Sci.,**11**, no. 1, 2011, p. 1730.
7.ORLOVSKII, V.P., KOMLEV, V.S., BARINOV, S.M., J. Inorg. Mater., **38**, no.10, 2002, p. 1159.
8.CHEN, Y., ZHANG, Y.Q., ZHANG, T.H., GAN, C.H., ZHENG, C.Y., YU, G., Carbon, **44**, 2006, p. 37.
9.RAMLI, R. A., ADNAN, R., BAKAR, M.A., MASUDI, S.M., J. Phys. Sci., **22**, no. 1, 2011, p. 25.
10.NEUENDORF, R.E., SAIZ, E., TOMSIA, A.P., RITCHIE, R.O., Acta Biomater. **4**, 2008, p. 1288.
11.HABRAKEN, W., WOLKE, J.G.C., JANSEN, J.A., Adv. Drug. Deliv. Rev., **59**, 2007, p. 234.
12.BONFIELD, W., KNOWLES, J.C., J. Biomed. Mater. Res., **27**, 1993, p. 1591.
13.PARK, K., VASILOS, T., J. Mater Sci. Lett., **16**, 1997, p. 985.
14.SIMMONS, T.J., LEE, S.-H., PARK, T.-J., HASHIM, D.P., AJAYAN, P.M,. LINDHARDT, R.J., Carbon, **47**, 2009, p. 1561.
15.KURAHATTI, R.V., SURENDRANATHAN, A.O., KORI, S.A., SINGH, N., RAMESH KUMAR., A.V., SRIVASTAVA, S., Defence Sci. J., **60**, no. 5, 2010, p. 551.
16.SAMBARKAR, P.P., PATWEKAR, S.L., DUDHGAONKAR, B.M., Int. J. Pharm. Pharm. Sci., **4**, no. 2, 2012, p. 60.
17.DE VOLDER, M.F.L., TAWFICK, S.H., BAUGHMAN, R.H., HART, A.J., Science , **339**, 2013, p. 535.
18.ARSECULARATNE, J.A., ZHANG, L.C., Recent Pat. Nanotechnol., **1**, 2007, p. 176.
19.SYAM SUNDAR, L., HAWALDAR, R., TITUS, E., GRACIO, J., SINGH, M.K., Biomedical Engineering – Technical Applications in Medicine, **5**, R.Hudak, M.Penhaker, J.Majernik Editors, InTech, Rjeka, 2012, p. 117-128, ISBN 978-953-51-0733-0, http://dx.doi.org/10.5772/48385
20.KWAADSTENIET, M., BOTES, M., CLOETE, T.E., Nano, **6**, 2011, p. 395.
21.GUPTA, P., LAHIRI, D., Neural Regen. Res., **11**, no. 7, 2016, p.1062.
22.LAHIRI, D., GHOSH, S., AGARWAL, A., Mater. Sci. Eng. C, **32**, no. 7, 2012, p. 1727.
23.MAN, I., PIRVU, C., DEMETRESCU, I., Rev. Chim. (Bucharest), **59**, no. 6, 2008, p. 615.
24.LAHIRI, I., LAHIRI, D., JIN, S., AGARWAL, A., CHOI, W., ACS Nano, **5**, no. 2, 2011, p. 780.
25.PRODANA, M., DUTA, M., IONITA, D., BOJIN, D., MIRUNA, D., STAN, S., DINISCHIOTU, A., DEMETRESCU, I., Ceram. Int., **41**,no. 5, 2015, p. 6318.
26.GOPI, D., SHINYJOY, E., SEKAR, M., SURENDIRAN, M., KAVITHA, L., SAMPATH KUMAR, T.S., Corros. Sci., **73**, 2013, p. 321.
27.LI, A., WANG, L., LI, M., XU, Z., LI, P., ZHANG, Z.Z., Dig. J. Nanomater. Biostruct., **9**, 2014, p. 599.
28.STOIAN, A.B., PIRVU, C., UPB Sci. Bull., series B, **75**, no. 2, 2013, p. 43.
29.TOTEA, G., IONITA, D., KATUNAR, R.M., CERE, S., DEMETRESCU, I., Dig J Nanomater. Bios., **9**, no. 2, 2014, p. 575.
30.TOTEA, G., IONITA, D., DEMETRESCU, I., MITACHE, M.M., Cent. Eur. J. Chem., **12** , 2014, p. 796.
31.KATO, J., KIM, H.-E., TAKIGUCHI, N., KURODA, A., OHTAKE, H., J. Biosci. Bioeng., **106**, no. 1, 2008, p. 1.
32.POLLITT, E.J.G., CRUSZ, S.A., DIGGLE, S.P., Sci. Rep., **5**, 2015, p.1.
33.ANSARI, M.A., KHAN, H.M., KHAN, A.A., MALIK, A., SULTAN, A., SHAHID, M., SHUJATULLAH, F., AZAM, A., Biol. Med., **3**, no. 2, 2011, p. 141.
34.MUT POPESCU, D., Hematologie clinica, Ed. a 2-a, Editura Medicala, Bucuresti, 1994, p. 1-282.
35.DOUNDOULAKIS, H., J. Prosthet. Dent., **58**, 1987, p. 471.
36.KUMAR, M.K., REDDY, A.L.M., RAMAPRABHU, S., Sens. Actuat. B, **130**, 2008, p. 653.
37.KATSIKOGIANNI, M, MISSIRLIS, Y.F., Eur. Cell. Mater., **8**, 2004, p. 37.
38.DONG, L., HENDERSON, A., FIELD, C., J. Nanotechnol., 2012, Article ID 928924, p. 1.
39.POURBAIX, M., Atlas of Electrochemical Equilibria in Aqueous Solutions, New York: Pergamon Press, 1966, p. 1-644.
40.WALSH, F.M., AMYES, S.G.B., Curr. Opin. Microbiol., **7**, no. 5, 2004, p. 439.
41.DONG, X, TANG, Y., LILLY, M., AFERCHICH, K., YANG, L., Nano Life, **2**, 2012, p. 1.
42.LOPEZ, D.A., DURAN, A., CERE, S.M., J. Mater.Sci. Mater. Med., **19**, no. 5, 2008, p. 2137.
43.KANG, S., PINAULT, M., PFEFFERLE, L.D., ELIMELECH, M., Langmuir, **23**, no. 17, 2007, p. 8670.
44.YACOBY, I., BENHAR, I., Nanomedicine, **3**, no. 3, 2008, p. 329.
45.AFERCHICH, K., LILLY, M., YANG, L., J. Nanosci. Nanotechnol., **12**, 2012, p. 3821.
46.KANG, S., HERZBERG, M., RODRIGUES, D.F., ELIMELECH, M., Langmuir, **24**, 2008, p. 6409.
47.CHEN, H., WANG, B., GAO, D., GUAN, M., ZHENG, L., OUYANG, H., FENG, W., Small, **9**, no. 16, 2013, p. 2735.
48.LI, H., YUAN, W.Z., CHEN, X., YANG, L., ZHAO, J., ZHANG, Y., J. Mater. Sci., **47**, 2012, p. 5030.

Manuscript received: 22.08.2017